© 2018. Published by The Company of Biologists Ltd | Journal of Cell Science (2018) 131, jcs210575. doi:10.1242/jcs.210575

SHORT REPORT

Phosphorylation of XIAP at threonine 180 controls its activity in Wnt signaling

Victoria H. Ng[1,*], Brian I. Hang[2,*], Leah M. Sawyer[2], Leif R. Neitzel[2], Emily E. Crispi[2], Kristie L. Rose[3], Tessa M. Popay[2], Alison Zhong[2], Laura A. Lee[4], William P. Tansey[2], Stacey Huppert[5] and Ethan Lee[1,2,6,‡]

ABSTRACT

X-linked inhibitor of apoptosis (XIAP) plays an important role in preventing apoptotic cell death. XIAP has been shown to participate in signaling pathways, including Wnt signaling. XIAP regulates Wnt signaling by promoting the monoubiquitylation of the co-repressor Groucho/TLE family proteins, decreasing its affinity for the TCF/Lef family of transcription factors and allowing assembly of transcriptionally active β-catenin–TCF/Lef complexes. We now demonstrate that XIAP is phosphorylated by GSK3 at threonine 180, and that an alanine mutant ($XIAP^{T180A}$) exhibits decreased Wnt activity compared to wild-type XIAP in cultured human cells and in *Xenopus* embryos. Although $XIAP^{T180A}$ ubiquitylates TLE3 at wild-type levels *in vitro*, it exhibits a reduced capacity to ubiquitylate and bind TLE3 in human cells. $XIAP^{T180A}$ binds Smac (also known as DIABLO) and inhibits Fas-induced apoptosis to a similar degree to wild-type XIAP. Our studies uncover a new mechanism by which XIAP is specifically directed towards a Wnt signaling function versus its anti-apoptotic function. These findings have implications for development of anti-XIAP therapeutics for human cancers.

KEY WORDS: GSK3, Wnt, XIAP, Apoptosis, Phosphorylation, Ubiquitylation

INTRODUCTION

Cellular inhibitor of apoptosis (cIAP) protein family members, which include XIAP, are well known for binding caspases and inhibiting their activities (Galbán and Duckett, 2010). XIAP has also been shown to have a critical role in Wnt signaling (Hanson et al., 2012). The Wnt signaling pathway plays an integral role in many developmental processes and in human cancer (Saito-Diaz et al., 2013). In the absence of a Wnt signal, cytoplasmic β-catenin is phosphorylated by casein kinase 1α (CK1α) and glycogen synthase kinase 3 (GSK3), and targeted for ubiquitin-mediated degradation by the proteasome. GSK3 is a serine/threonine kinase that has been shown to be involved in multiple signaling pathways, including insulin and Hedgehog signaling (Wu and Pan, 2010). Upon Wnt activation, β-catenin accumulates in the cytoplasm, translocates into the nucleus and displaces members of the co-repressor Groucho/TLE (Gro/TLE) family from members of the TCF/Lef transcription factor family to initiate a Wnt transcriptional program (Daniels and Weis, 2005). We previously demonstrated that XIAP associates with the co-repressor complex to promote monoubiquitylation of Gro/TLE proteins, thereby decreasing its affinity for TCF proteins and allowing β-catenin to bind these transcription factors (Hanson et al., 2012). How XIAP is recruited to Gro/TLE and how its activity is regulated during Wnt signaling versus during apoptosis is unknown. We now demonstrate that XIAP binds and is phosphorylated by GSK3 at threonine 180; this phosphorylation event is required for its activity in Wnt signaling, but is dispensable for its role in the apoptotic pathway.

RESULTS AND DISCUSSION

XIAP is a substrate of GSK3 *in vitro*

A previous study has demonstrated that XIAP interacts with GSK3 in mammalian cells (Sun et al., 2009). Consistent with this result, we also showed that endogenous GSK3 co-immunoprecipitates with endogenous XIAP in several cultured cell lines, including the colorectal cancer lines SW480 and HCT116 (Fig. 1A; Fig. S1A). We found, however, that this interaction was not altered upon active Wnt signaling. We previously demonstrated that Wnt signaling did not alter the overall level of XIAP or its intracellular localization and only a small, localized pool of XIAP associated with TCF proteins is affected (Hanson et al., 2012). Thus, the interaction between XIAP and GSK3 may be regulated similarly at a localized level. We found that XIAP was phosphorylated by GSK3 in an *in vitro* radioactive kinase assay (Fig. 1B; Fig. S1B). Certain GSK3 substrates require a previous (primed) phosphorylation on a serine or threonine residue (Beurel et al., 2015). We therefore tested whether previous phosphorylation by CK1 could enhance the phosphorylation of XIAP by GSK3. Prior incubation with CK1 (under *in vitro* kinase conditions) dramatically increased the phosphorylation of purified XIAP by GSK3 (Fig. 1C). This result suggests that CK1 (or possibly another kinase) may prime XIAP for GSK3 phosphorylation.

The online systems biology resource tool PhosphoSitePlus (Hornbeck et al., 2015) curates various data sources to provide information on protein phosphorylation sites. Using this resource, we searched for previously reported phosphorylation sites on XIAP (Fig. 1D). To determine whether any of these sites represent actual GSK3 phosphorylation sites on XIAP, we performed an *in vitro* kinase reaction with purified XIAP and GSK3 followed with liquid chromatography-mass spectrometry (LC-MS) analysis. One of the predicted sites, threonine 180 (T180), which is located within the BIR2 domain of XIAP, is phosphorylated by GSK3 *in vitro* (Fig. S1C). This result is consistent with previous studies demonstrating that XIAP is phosphorylated on T180 in human cells (Mertins et al., 2016; Sharma et al., 2014).

[1]Program in Cancer Biology, Vanderbilt University, Nashville, TN 37232, USA. [2]Department of Cell & Developmental Biology, Vanderbilt University, Nashville, TN 37232, USA. [3]Vanderbilt Mass Spectrometry Research Center Proteomics Core, Nashville, TN 37232, USA. [4]Department of Pathology, Microbiology, and Immunology, Vanderbilt University Medical Center, Nashville, TN, USA. [5]Division of Gastroenterology, Hepatology, and Nutrition, Cincinnati Children's Hospital Medical Center, Cincinnati, OH 45229, USA. [6]Vanderbilt Ingram Cancer Center, Vanderbilt Medical Center, Nashville, TN 37232, USA.
*These authors contributed equally to this work

‡Author for correspondence (ethan.lee@vanderbilt.edu)

V.H.N., 0000-0003-2344-8468; B.I.H., 0000-0003-4591-4466; A.Z., 0000-0003-4868-7406; E.L., 0000-0001-8405-6156

Received 4 September 2017; Accepted 16 April 2018

Journal of Cell Science (2018) 131, jcs210575. doi:10.1242/jcs.210575

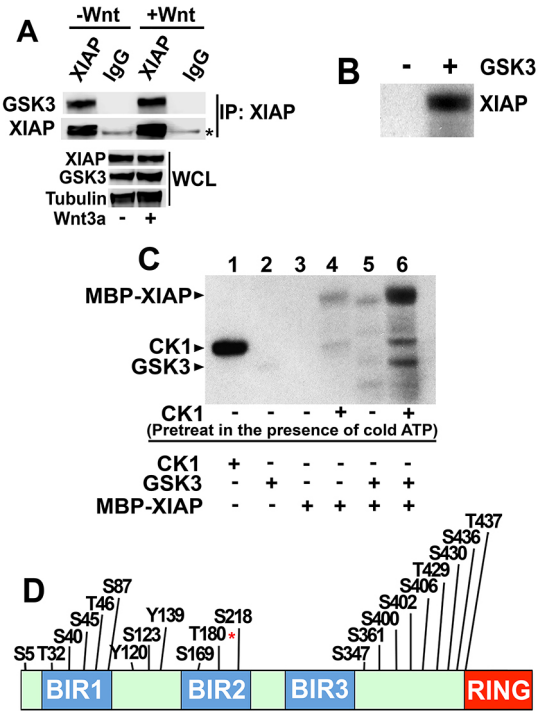

Fig. 1. XIAP is phosphorylated by GSK3 at T180. (A) Endogenous XIAP co-immunoprecipitates with endogenous GSK3. XIAP was immunoprecipitated (IP) from whole-cell lysates (WCL) of HEK293STF cells incubated in the absence or presence of recombinant Wnt3a followed by immunoblotting. The asterisk indicates the heavy chain of IgG. (B) Purified XIAP is phosphorylated by GSK3 *in vitro* in a [γ^{32}P]ATP kinase assay. Reactions were analyzed by SDS/PAGE followed by autoradiography. (C) CK1 enhances XIAP phosphorylation by GSK3. XIAP bound to beads was incubated with CK1 in a kinase reaction containing non-radioactive (cold) ATP (lanes 4 and 6). CK1 was washed away and XIAP-bound beads incubated with GSK3 in a kinase reaction containing [γ^{32}P]ATP. Reactions were analyzed by SDS/PAGE followed by autoradiography. Kinase only lanes show CK1 and GSK3 autophosphorylation (lanes 1 and 2). Results in A–C were replicated at least three times. (D) The predicted phosphorylation site at T180 of XIAP is an *in vitro* GSK3 phosphorylated site. Predicted phosphorylation sites on XIAP were curated by the PhosphoSitePlus online resource tool (Hornbeck et al., 2015). LC-MS analysis of XIAP identifies T180 (asterisk) as a prominent *in vitro* GSK3 phosphorylation site.

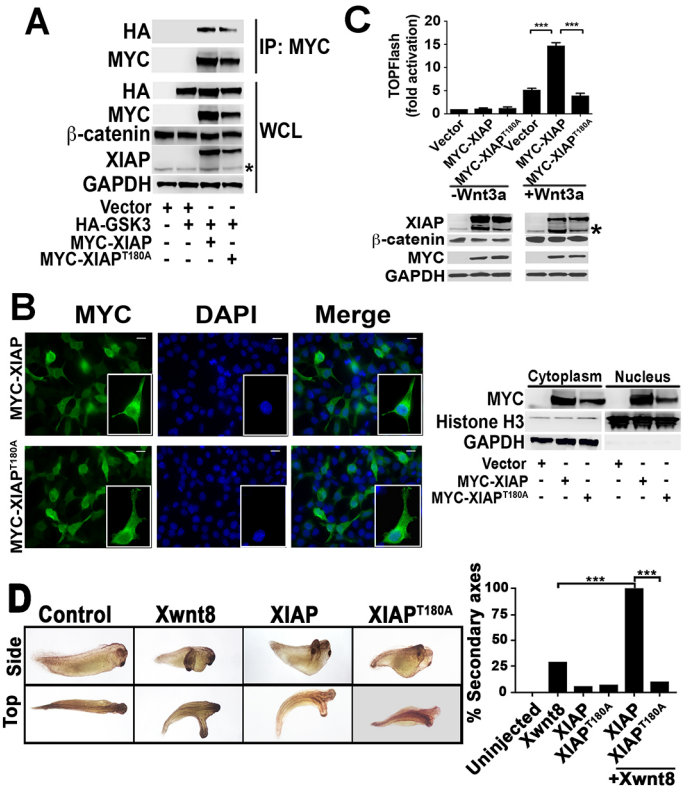

Fig. 2. The XIAP^{T180A} mutant exhibits decreased Wnt activity compared to wild-type XIAP in cultured human cells and in *Xenopus* embryos. (A) GSK3 associates with XIAP and the kinase mutant, XIAP^{T180A}, to a similar extent. HEK293STF cells were transfected with vector, HA–GSK3, MYC–XIAP and MYC-XIAP^{T180A} as indicated, whole cell lysates (WCL) were collected, and immunoprecipitation (IP) performed with anti-MYC antibody. The asterisk indicates endogenous XIAP. (B) The XIAP^{T180A} mutant does not exhibit a localization that is distinct from XIAP. Left, HEK293STF cells were transfected with MYC–XIAP or MYC–XIAP^{T180A}, fixed, and immunostained for MYC and DNA (DAPI). Scale bars: 12.5 µm. Right, cytoplasmic and nuclear fractionations were isolated from transfected cells and immunoblotted for MYC, Histone H3 (a nuclear marker) and GAPDH (a cytoplasmic marker). (C) In contrast to wild-type XIAP, XIAP^{T180A} does not potentiate Wnt3a signaling. HEK293STF cells were transfected with vector, MYC–XIAP or MYC–XIAP^{T180A} as indicated, for 24 h, and cells incubated in the absence or presence of recombinant Wnt3a for 24 h. The asterisk indicates endogenous XIAP. Graph shows mean±s.d. of TOPflash activation normalized to the cell titer. ***P<0.0001 (one-tailed Student's *t*-test). All experiments were repeated at least three times. (D) The XIAP^{T180A} mutant does not potentiate Wnt8 (Xwnt8)-induced axis formation in *Xenopus* embryos, in contrast to wild-type XIAP. Embryos (four-cell stage) were injected ventrally with control, *XIAP*^{T180A} or *XIAP* mRNA (2 ng each) with or without *Wnt8* mRNA (0.1 ng) and allowed to develop. Representative *Wnt8*-, *XIAP*- and *XIAP*^{T180A}-injected embryos are on the left. The percentage of embryos with secondary axis formation is shown on the right (n≥31 per group). ***P<0.0001 (Fisher's exact test, with Bonferroni correction). All results were replicated at least three times.

The XIAP^{T180A} phosphomutant exhibits decreased Wnt activity

We next tested whether an alanine mutant of XIAP at position T180 (XIAP^{T180A}) co-immunoprecipitated with GSK3 to a similar extent to wild-type XIAP (Fig. 2A), and found that the interaction was similar. The XIAP ligase mutant XIAP$^{H467A/F495A}$ (Gyrd-Hansen et al., 2008; Holley et al., 2002; Damgaard et al., 2012) also co-immunoprecipitated with GSK3 to a similar extent to wild-type XIAP (Fig. S2A), suggesting that the interaction between XIAP and GSK3 does not depend on the ligase activity of XIAP. We next performed immunolocalization of XIAP^{T180A} to determine whether it exhibited a different localization pattern compared to wild-type XIAP. We transfected MYC-tagged XIAP and XIAP^{T180A} into HEK293STF cells and performed immunostaining (Fig. 2B). We found no differences between the cellular localization of XIAP and XIAP^{T180A} as assessed by immunofluorescence. These results were confirmed by cytoplasmic and nuclear cellular fractionation studies of HEK293STF cells expressing XIAP or XIAP^{T180A} (Fig. 2B).

Consistent with our previous studies, we found that overexpression of XIAP is insufficient to promote Wnt activation in cultured human cells (Fig. 2C). Thus, XIAP is unlikely to be a limiting component of the Wnt signal transduction pathway in mammalian cells (Hanson et al., 2012). Similarly, we did not detect Wnt activity when we overexpressed XIAP^{T180A} (Fig. 2C). We next tested whether XIAP could become limiting when the Wnt pathway is activated. Using HEK293STF cells, which contain a stably integrated luciferase-based Wnt reporter (Veeman et al., 2003), we found that overexpression of XIAP potentiates activation by Wnt3a (Fig. 2C). The lack of change in β-catenin levels in the XIAP (or XIAP^{T180A}) plus Wnt3a condition compared to that seen upon

Wnt3a treatment alone is consistent with the nuclear function of XIAP (which acts downstream of the β-catenin destruction complex and would not be expected to impact steady-state β-catenin levels) (Hanson et al., 2012). In contrast to what was seen with XIAP, we found no enhancement of Wnt reporter activity upon overexpression of XIAP^{T180A} (Fig. 2C; Fig. S2B), suggesting that phosphorylation at the T180 site is critical for the role of XIAP during Wnt signaling.

The XIAP^{T180A} phosphomutant exhibits reduced capacity to potentiate Wnt8 activity in *Xenopus* embryos

Dorsal-anterior structure formation in *Xenopus laevis* embryos is regulated by Wnt signaling (Heasman, 2006), and induction of secondary axis formation in *Xenopus* embryos represents a powerful readout for Wnt signaling *in vivo*. We previously demonstrated that morpholino knockdown of XIAP resulted in severely ventralized *Xenopus* embryos, while injection of XIAP mRNA induced secondary axis formation, consistent with a positive role for XIAP in Wnt signaling (Hanson et al., 2012). The latter result suggests that XIAP is a limiting factor in the developing *Xenopus* embryo. We found that *XIAP^{T180A}* induced secondary axis formation to a similar extent to *XIAP* (Fig. 2D,E). Immunoblotting confirmed that XIAP^{T180A} and XIAP were expressed at similar levels in the injected embryos (Fig. S2C). *XIAP* synergizes with *Wnt8* mRNA to induce axis formation in *Xenopus* embryos. In contrast, *XIAP^{T180A}* co-injection with *Wnt8* mRNA resulted in a lower percentage of embryos with duplicated axes versus what was seen upon *Wnt8* injection alone. Thus, the XIAP^{T180A} phosphomutant has impaired capacity to potentiate Wnt signaling.

The XIAP^{T180A} phosphomutant exhibits decreased capacity to bind and ubiquitylate TLE3

We previously demonstrated that XIAP monoubiquitylates TLE3 *in vitro* and in cultured mammalian cells. To test whether the decreased capacity of XIAP^{T180A} to potentiate Wnt signaling is due to its incapacity to ubiquitylate Gro/TLE proteins, we tested the capacity of XIAP^{T180A} to ubiquitylate TLE3 in an *in vitro* ubiquitylation assay. We found that XIAP^{T180A} ubiquitylates TLE3 to a similar degree to wild-type XIAP (Fig. 3A). This result suggests that XIAP^{T180A} does not have reduced intrinsic catalytic activity when compared to wild-type XIAP. In contrast, in cell-based ubiquitylation assays, the XIAP^{T180A} phosphomutant exhibited decreased capacity to ubiquitylate TLE3 when compared to wild-type XIAP (Fig. 3B). As a control, we could show that the ligase mutant XIAP$^{H467A/F495A}$ exhibited a reduced capacity (similar to control transfection) to ubiquitylate TLE3 compared to wild-type XIAP (Fig. S3A). Addition of the proteasome inhibitor, MG132, resulted in enhanced ubiquitylation of the XIAP$^{H467A/F495A}$ mutant itself (Fig. S3B), suggesting that the decreased activity of the XIAP$^{H467A/F495A}$ mutant may be, in part, due to its rapid turnover.

We found a reduced interaction between XIAP^{T180A} and TLE3 when compared to XIAP and TLE3, as assessed by co-immunoprecipitation assays. Wnt3a treatment did not significantly enhance the interaction between TLE3 and XIAP^{T180A} or XIAP (Fig. 3C). These results suggest that the decreased capacity of XIAP^{T180A} to ubiquitylate TLE3 in cultured cells is due, in part, to its decreased binding to TLE3.

The anti-apoptotic activity of XIAP^{T180A} is indistinguishable from that of wild-type XIAP

We next asked whether XIAP^{T180A} has reduced activity in the apoptotic pathway. One of the best-characterized substrates of XIAP is second mitochondria-derived activator of caspases (Smac; also known as DIABLO) (MacFarlane et al., 2002). We found that XIAP^{T180A} interacted with Smac to a similar extent to wild-type XIAP (Fig. 4A). Overexpression of XIAP inhibits apoptosis in cultured cells (Suzuki et al., 2001). We thus tested whether overexpressed XIAP^{T180A} inhibits Fas ligand-induced apoptosis in HeLa cells (Ashkenazi and Dixit, 1998). There was no observable difference in the capacity of MYC–XIAP or MYC–XIAP^{T180A} to inhibit Fas ligand-induced apoptosis in HeLa cells (Fig. 4B). Thus, phosphorylation of XIAP at the T180 site is required for the full activity of XIAP in the Wnt pathway, but not in the apoptotic pathway.

How the Wnt transcriptional complex is converted from a repressor complex into an activator complex is not well understood. Upon Wnt activation, XIAP is recruited onto Wnt target gene promoters to ubiquitylate Gro/TLE proteins bound to TCF/Lef proteins, decreasing their affinity for these proteins (Hanson et al., 2012). In the same study, we showed that XIAP interacts with Gro/TLE proteins in the absence or presence of Wnt stimulation, and we speculated that XIAP also decreases the pool of free Gro/TLE proteins that can interact with TCF/Lef proteins to inhibit transcription. Thus, Wnt signaling regulates XIAP activity by promoting its recruitment to the TCF/Lef transcriptional complex where it ubiquitylates TCF/Lef proteins bound to Gro/TLE proteins. We now demonstrate that XIAP is phosphorylated by GSK3, which could mediate this process. This result confirms data curated by PhosphoSitePlus from genome-scale proteomic studies indicating

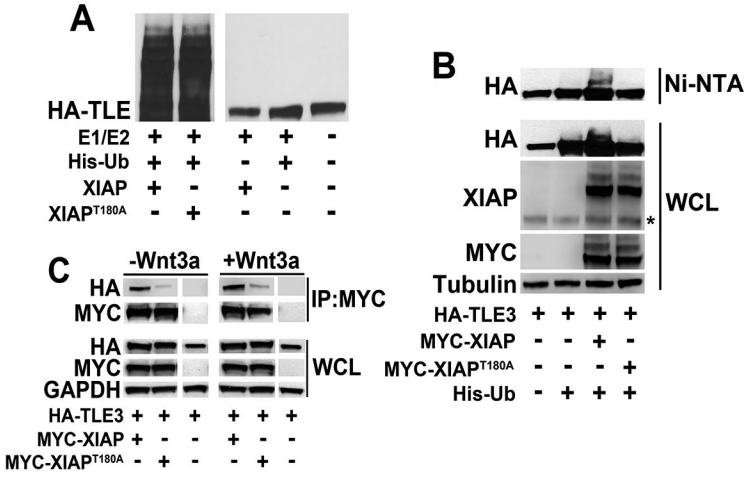

Fig. 3. The XIAP^{T180A} mutant shows decreased binding and ubiquitylation of TLE3. (A) XIAP^{T180A} ubiquitylates TLE3 to a similar extent to wild-type XIAP *in vitro*. *In vitro*-translated HA–TLE3 was incubated in an *in vitro* ubiquitylation reaction containing recombinant E1/E2, ubiquitin, and XIAP or XIAP^{T180A}. Ubiquitylated TLE3 was visualized by immunoblotting with anti-HA antibody. (B) XIAP^{T180A} exhibits reduced capacity to ubiquitylate TLE3 in cultured human cells compared to wild-type XIAP. HEK293STF cells were transfected as indicated, lysed under denaturing conditions, and His-Ub-modified proteins isolated by nickel affinity chromatography. XIAP and TLE3 were detected by immunoblotting with anti-MYC and anti-HA antibodies, respectively. The asterisk indicates endogenous XIAP. WCL, whole-cell lysates. (C) XIAP^{T180A} exhibits decreased affinity for HA–TLE3 compared to wild-type XIAP. HEK293STF cells were transfected for 24 h as indicated followed by incubation in the absence or presence of recombinant Wnt3a for 24 h. Lysates were collected and immunoprecipitated (IP) with anti-MYC antibody. Co-immunoprecipitated HA–TLE3 was detected by anti-HA antibody. All results were replicated at least three times.

Journal of Cell Science (2018) 131, jcs210575. doi:10.1242/jcs.210575

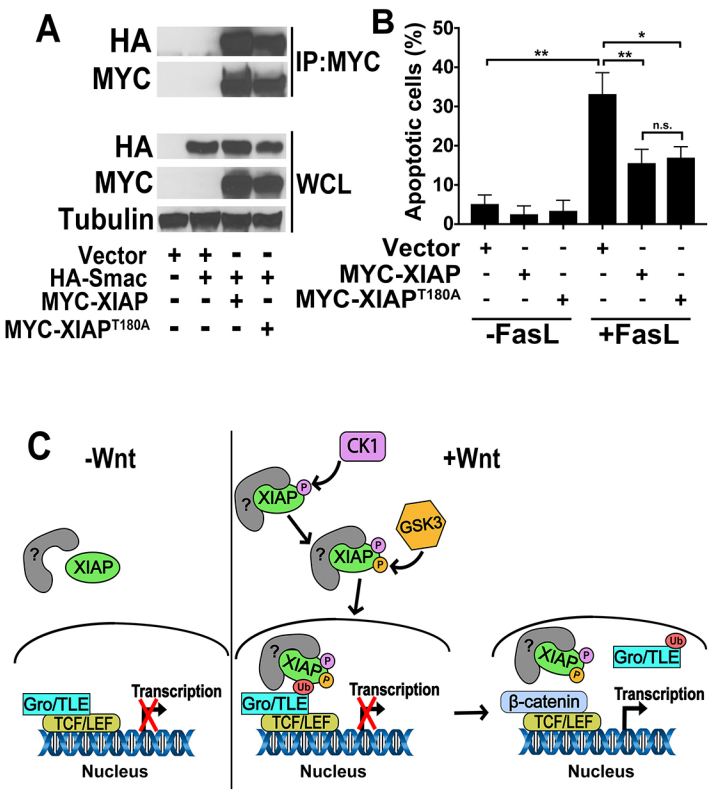

Fig. 4. In contrast to its activity in the Wnt pathway, XIAP^{T180A} has a similar activity to that of wild-type XIAP in the apoptotic pathway. (A) Smac co-immunoprecipitates (IP) with XIAP and XIAP^{T180A} to a similar extent. HEK293STF cells were transfected as indicated with vector or HA–Smac plus MYC–XIAP or MYC–XIAP^{T180A}. Lysates were collected and immunoprecipitation performed with anti-MYC antibody followed by immunoblotting with anti-HA antibody. WCL, whole cell lysates. Results were replicated at least three times. (B) Overexpression of XIAP and XIAP^{T180A} decreases the percentage of Fas ligand (FasL)-induced apoptosis to a similar extent. HeLa cells were transfected for 24 h as indicated and incubated in the absence or presence of recombinant Fas ligand (100 ng/ml) for 24 h. Cells were then stained with Annexin V and propidium iodide. Graph shows the mean±s.d. of percentage of apoptotic cells. Data was analyzed and processed using FlowJo. **P<0.001, *P<0.01; n.s., not significant (one-tailed Student's t-test). All experiments were repeated at least three times. (C) A model for the regulation of XIAP activity in the Wnt pathway by phosphorylation at position T180. See text for more information.

that XIAP is phosphorylated on T180 in human cells, although the significance of XIAP T180 phosphorylation was not clear (Mertins et al., 2016; Sharma et al., 2014). Our current data suggest that phosphorylation of T180 is required for full Wnt activation. Unfortunately, given the likely small pool of phosphorylated nuclear XIAP involved in Wnt signaling, we were unable to detect this form of XIAP in cell extracts by using conventional biochemical methods. The development of a phospho-T180 specific antibody would be a powerful tool to further assess the *in vivo* importance of this phosphorylated form of XIAP.

One possible model is that the interaction between XIAP and Gro/TLE proteins is facilitated by an as-yet-unidentified factor due to phosphorylation of XIAP at T180 by GSK3 (Fig. 4C). This model may explain why overexpression of XIAP^{T180A} does not potentiate Wnt signaling, as it would be incapable of binding Gro/TLE proteins and instead would act to sequester the unknown factor. It is not clear how phosphorylation of XIAP by GSK3 is regulated by Wnt signaling given that XIAP binds to GSK3 irrespective of Wnt activation (Sun et al., 2009 and our data). One possibility is that Wnt signaling either promotes phosphorylation of XIAP on the appropriate site(s) or primes the GSK3 site(s) on XIAP via regulation of another kinase (e.g. CK1). The latter possibility is particularly attractive given that CK1 has been shown to prime GSK3 sites on both β-catenin and LRP6 to inhibit and activate Wnt signaling, respectively (Liu et al., 2002; Zeng et al., 2005). One potential priming phosphorylation site for GSK3 is S186. Although the optimal distance between a primed site and a GSK3 target is four amino acids, greater distances have also been demonstrated (Cole et al., 2004).

Beyond its role in apoptosis, there is increasing evidence that XIAP can participate in a variety of signaling pathways. For example, in addition to our previous studies demonstrating the role of XIAP in the Wnt pathway, a number of studies have shown that XIAP overexpression is also capable of activating the nuclear factor (NF)-κB pathway (Barkett et al., 1997). How XIAP is recruited differentially to regulate NF-κB and/or Wnt signaling, as opposed to its apoptotic function has remained a mystery. Future studies would need to include CRISPR/Cas9-mediated editing of the T180 site in the endogenous XIAP gene to answer this question. Finally, it would be interesting to determine the role of additional post-translational modifications (e.g. ubiquitylation and sumoylation) on the activity of XIAP in other signaling pathways and apoptosis.

MATERIALS AND METHODS

Plasmids

pCS2-MYC-XIAP, pMAL-XIAP and pGEX-TEV-GST were constructed as previously described (Hanson et al., 2012). The following plasmids were gifts: pMT107-His-Ub (William Tansey, Vanderbilt University, Nashville, TN) and pCDNA.3-HA-TLE3 (Andreas Kispert, Hannover Medical School, Hanover, Germany). pCS2-MYC-XIAP^{T180A}, pMAL-XIAP^{T180A} and pCS2-MYC-XIAP$^{H467A/F495A}$ were generated using PCR-based mutagenesis techniques as previously described (Laible and Boonrod, 2009) using the following primers: forward, 5′-GGCCAGACTATGCTCACCTAGCCCCAAGAGAG-3′ and reverse 5′-CTCTCTTGGGGCTAGGTGAGCATAGTCTGGCC-3′ for XIAP^{T180A}; forward 5′-CATTGTTTACAAGTGACTAGAGCTCCACAAGGAACAAAAACGATAGC-3′ and reverse 5′-GCTATCGTTTTTGTTCCTTGTGGAGCTCTAGTCACTTGTAAACAATG-5′, then forward 5′-GGCGCGCCTTAAGACATAGCAATTTTTTGCTTGAAAGTAATGACTGTGTAGC-3′ and reverse 5′-GCTACACAGTCATTACTTTCAAGCAAAAAATTGCTATGTCTTAAGGCGCGCC-3′ for XIAP$^{H467A/F495A}$.

Cell lines

HEK293STF was a gift from the laboratory of Jeremy Nathans (Department of Molecular Biology and Genetics, Johns Hopkins University, MD). HCT116 was a gift from the laboratory of Bert Vogelstein (Sidney Kimmel Comprehensive Cancer Center, Johns Hopkins University, MD). SW480 and HeLa were purchased from ATCC (CCL-228, CCL-2). The cells lines used were fresh stocks from liquid nitrogen, and were, thus, not contaminated.

Antibodies

The following antibodies were used: rabbit anti-XIAP (3:200 for immunoprecipitation, cat. no. NB100-56185, Novus Biologicals, Littleton, CO), mouse anti-XIAP (1:1000, cat. no. 610716, BD Transduction, San Jose, CA), rat anti-HA (1:1000, cat. no. 11867423001, Roche, Basel, Switzerland), mouse anti-MYC (1:1000, Vanderbilt Antibody and Protein Resource, Nashville, TN), mouse anti-GAPDH (1:5000, cat. no. sc-47724, Santa Cruz Biotechnology, Dallas, TX), mouse anti-GAPDH (1:500, cat. no. DSHB-hGAPDH-2G7, DSHB, Iowa City, IA), rabbit anti-Histone H3 (1:2500, cat. no. sc-10809, Santa Cruz Biotechnology), mouse anti-β-catenin (1:5000, cat. no. 610153, BD Transduction), mouse anti-GSK3β (1:1000, cat. no. 610202, BD Transduction), rabbit IgG (Santa Cruz Biotechnology), goat anti-mouse-IgG conjugated to horseradish peroxidase (HRP; 1:5000, Promega, Madison, WI) and goat anti-rabbit-IgG conjugated to HRP (1:5000, Promega).

Expression and purification of XIAP

BL21 bacterial cells transformed with MBP–XIAP or MBP–XIAP^{T180A} plasmids were grown in a 37°C shaking incubator until cell density reached an optical density at 600 nm (OD_{600})=0.5. IPTG (300 µM) was then added and the cultures incubated at 18°C overnight. Cells were then spun down, and cell pellets lysed by sonication in Tris-NaCl-phenylmethylsulfonyl fluoride (TNP) buffer (50 mM Tris-HCl, 150 mM NaCl, 2 mM EDTA, 1 mM PMSF and 0.1% Triton X-100). Lysates were centrifuged at 16,000 ***g*** at 4°C for 10 min, and supernatants incubated with amylose beads on a shaking platform for 2 h at 4°C. Beads were then washed three times with 10× column volumes of TNP, and MBP-bound proteins were eluted with TNP buffer containing 1% maltose. Eluted proteins were further purified on a Mono Q anion-exchange column using the AKTA FPLC apparatus (GE Healthcare, Marlborough, MA). Fractions containing the MBP fusion proteins were concentrated to 1 mg/ml by using Amicon Ultra centrifugal filter units (EMD Millipore, Billerica, MA), and proteins were aliquoted and stored at −80°C until use.

Immunoblotting and immunoprecipitation assays

For immunoblotting of whole-cell lysate, cells were lysed in non-denaturing lysis buffer [NDLB; 100 mM Tris-HCl pH 7.5, 500 mM NaCl, 5 mM EDTA, 1% (v/v) Triton X-100 and 1 mM PMSF], centrifuged at 16,000 ***g*** for 10 min at 4°C, and supernatants were collected for SDS-PAGE. Imaging was performed with c-DIGIT (LI-COR, Lincoln, NE) and X-ray film. For immunoblotting of fractionated cells, cells were lysed and fractions collected as previously described prior to SDS-PAGE (Thorne et al., 2010). For immunoprecipitation assays, cells were lysed in NDLB plus ubiquitin aldehyde (250 ng/µl) for samples expressing HA–TLE3 and MYC–XIAP constructs. For all other samples, 1 mM PMSF, 1× PhosSTOP (Roche), 1 mM NaF and 1 mM Na_3VO_4 were added. Lysates were centrifuged at 16,000 ***g*** for 10 min at 4°C, and anti-MYC agarose beads (Sigma-Aldrich, St Louis, MO), anti-XIAP antibody (Novus Biologicals) or anti-MYC antibody (Bethyl, Montgomery, TX) was added to the supernatant and incubated overnight at 4°C. For anti-XIAP and anti-MYC antibody samples, protein G beads (NEB, Ipswich, MA) were added and samples incubated for 1 h at 4°C. Beads were washed five times with 10× bead volumes of NDLB, bound proteins were eluted with sampler buffer and samples were processed for SDS-PAGE/immunoblotting.

Immunofluorescence

HEK293STF cells were grown on coverslips coated with fibronectin, fixed in 4% formaldehyde and permeabilized. Samples were then incubated with primary antibody followed by secondary antibodies conjugated to Alexa Fluor 488 (goat anti-mouse IgG H+L Alexa Fluor 488, cat. no. A-11001, ThermoFisher Scientific). Samples were mounted in ProLong Gold with DAPI (Invitrogen, Carlsbad, CA), and cells were visualized using a Cascade 512B camera mounted on a Nikon Eclipse TE2000-E confocal microscope.

In vitro phosphorylation assay

For the radioactive kinase assay, 100 ng MBP–XIAP was incubated with 100 ng TEV protease plus 250 units of GSK3 (NEB), 5 mM of cold ATP and 5 µCi of [γ^{32}P]ATP in 1× kinase reaction buffer [50 mM Tris-HCl pH 7.5, 10 mM $MgCl_2$, 5 mM dithiothreitol (DTT)]. Reactions were incubated at 30°C for 1 h on a TOMY shaker and terminated with sample buffer. For CK1 potentiation assays, 20 µl of MBP–XIAP (∼1 mg/ml) bound to amylose beads in 1× protein kinase buffer (NEB) containing ATP (1.5 mM) was incubated in the absence or presence of 110 ng recombinant CK1α (Thermo Fisher Scientific). Reactions were incubated at 30°C for 1 h on a TOMY shaker. Beads were then washed three times with 1× kinase reaction buffer prior to the GSK3 radioactive kinase assay.

Mass spectrometry analysis

A kinase reaction was performed as described for the *in vitro* phosphorylation reaction except that radioactive ATP was not added. Reactions were subjected to SDS-PAGE followed by staining with Coomassie Brilliant Blue. The band corresponding to XIAP was then excised and cut into 1 mm^3 pieces prior to in-gel digestion and analysis by liquid chromatography-coupled tandem mass spectrometry. The gel pieces were treated with 45 mM DTT and available cysteine residues were carbamidomethylated with 100 mM iodoacetamide. After destaining the gel pieces with 50% MeCN in 25 mM ammonium bicarbonate, proteins were digested with trypsin (10 ng/µl) in 25 mM ammonium bicarbonate overnight at 37°C. Peptides were extracted by gel dehydration (60% MeCN and 0.1% TFA), the extract was dried by speed vac centrifugation, and peptides were reconstituted in 0.1% formic acid. The peptide solutions were then loaded onto a capillary reverse phase analytical column (360 µm outer diameter ×100 µm internal diameter) using an Eksigent NanoLC HPLC and autosampler. The analytical column was packed C18 reverse phase resin (Jupiter, 3 µm beads, 300 Å, Phenomenox), directly into a laser-pulled emitter tip. Mobile phase solvents consisted of 0.1% formic acid, 99.9% water (solvent A) and 0.1% formic acid, 99.9% acetonitrile (solvent B). A 90-min gradient was performed, and eluting peptides were mass analyzed on an LTQ Orbitrap mass spectrometer (Thermo Scientific), equipped with a nanoelectrospray ionization source. The instrument was operated using a data-dependent method with dynamic exclusion enabled. Full scan (*m/z* 400–2000) spectra were acquired with the Orbitrap spectrometer, and the top five most abundant ions in each MS scan were selected for fragmentation via collision-induced dissociation (CID) in the LTQ. An isolation width of 2 *m/z*, activation time of 30 ms and 35% normalized collision energy were used to generate tandem mass spectra. Dynamic exclusion duration was set to 60 s. For identification of peptides, tandem mass spectra were searched with Sequest (Thermo Fisher Scientific) against a human subset database created from the UniprotKB protein database (www.uniprot.org). Variable modifications of +57.0214 on Cys (carbamidomethylation), +15.9949 on Met (oxidation), and +79.9663 on Ser, Thr and Tyr (phosphorylation) were included for database searching. Search results were assembled using Scaffold 4.3.2 (Proteome Software).

TOPFlash reporter assay

HEK293STF cells stably transfected with a luciferase-based Wnt reporter were incubated with Wnt3a-conditioned or control medium at 24 h post transfection. After 48 h, cells were lysed with 1× Passive Lysis Buffer (Promega) and luciferase activity determined with the Steady-Glo reagent following the manufacturer's instructions (Promega). CellTiter-Glo (Promega) was used to normalize luciferase activities. Statistical analysis was performed using a Student's *t*-test (one-tailed) in PRISM. A value of $P<0.05$ was considered statistically significant.

Xenopus axis duplication assay and immunoblotting embryos

Xenopus embryos were *in vitro* fertilized, de-jellied, cultured, and injected with mRNA as previously described (Peng, 1991). Embryos were assessed for complete or partial duplication, and statistical analyses were performed using Fisher's exact test with Bonferroni correction. A value of $P<0.05$ was considered statistically significant. For immunoblotting, sample buffer was added to pooled embryos from each condition and processed for SDS-PAGE. All animal studies were approved by the Institutional Animal Care and Use Committee (IACUC) at Vanderbilt University and were in accordance with their policies.

Ubiquitylation assays

In vitro ubiquitylation assays were carried out using the ubiquitin thioester/conjugation initiation kit (Boston Biochem, Cambridge, MA). Briefly, an E1 ubiquitin-activating enzyme (1 µg), E2 UbcH5a (1 µg), ubiquitin (1 µg), XIAP or XIAP^{T180A} (1 µg) and HA–TLE3 (2 µl, generated from an *in vitro* transcription-translation reaction, Promega) were assembled in a 20 µl reaction, and samples were incubated on a TOMY shaker at 30°C for 90 min. Reactions were terminated by addition of sample buffer, and ubiquitylated TLE3 products subjected to SDS-PAGE followed by immunoblotting for HA (Muratani and Tansey, 2003). For cell-based ubiquitylation assays, HEK293STF cells were transfected with plasmids encoding HA–TLE3, MYC–XIAP (or MYC–XIAP^{T180A} or MYC–XIAP$^{H467A/F495A}$) and His$_6$–ubiquitin, and treated with 100 µM MG132 for 4 h prior to the assay. The assays were performed using the His-tagged ubiquitin method as previously described (Salghetti et al., 1999).

Flow cytometry

HeLa cells were transfected with vector only, or MYC–XIAP or MYC–XIAP^{T180A}. Medium [DMEM (CellGro-Corning, MT10013CV) plus 10% FBS] was changed 24 h post transfection, and cells were incubated with 100 ng/ml recombinant Fas ligand (Sigma-Aldrich) for 24 h. Cells were released into the medium and adherent cells were counted, pelleted at 400 ***g*** and resuspended in ice-cold 1× staining medium (1× PBS, 2% BSA and 0.1% sodium azide). Cells (1×10^6) were then washed 2× in ice-cold 1× staining medium, resuspended in 200 µl of Annexin V-binding buffer (BioLegend, San Diego, CA) and stained with 2.5 µl Annexin V (BioLegend) plus 0.5 µl propidium iodide (1 mg/ml) for 15 min in the dark at room temperature. An additional 300 µl of Annexin V-binding buffer was added prior to analysis on a BD Fortessa cell analyzer. Data were analyzed with FlowJo software and PRISM.

Acknowledgements

The authors would like to thank the Tansey lab, the Lee lab and the Vanderbilt Mass Spectrometry Research Center Proteomics Core for helpful discussions.

Competing interests

Ethan Lee is cofounder of StemSynergy Therapeutics Inc., a company that is currently developing inhibitors of the Wnt pathway as potential chemotherapeutic agents.

Author contributions

Conceptualization: V.H.N., B.I.H., E.L.; Methodology: V.H.N., B.I.H., L.M.S., L.R.N., E.E.C., K.L.R., A.Z., E.L.; Validation: V.H.N., B.I.H., E.E.C., K.L.R.; Formal analysis: V.H.N., B.I.H., L.R.N., E.E.C., K.L.R., A.Z.; Investigation: V.H.N., B.I.H., L.M.S., L.R.N., E.E.C., K.L.R., T.M.P., A.Z., E.L.; Resources: W.P.T., E.L.; Data curation: V.H.N., B.I.H.; Writing - original draft: V.H.N., E.L.; Writing - review & editing: V.H.N., L.A.L., S.H., E.L.; Visualization: V.H.N., B.I.H., L.M.S., L.R.N., K.L.R.; Supervision: W.P.T., E.L.; Project administration: E.L.; Funding acquisition: E.L.

Funding

V.H.N. was supported by the National Institutes of Health Microenvironment Influences in Cancer Training Grant (T32 CA00959228). L.R.N. was supported by the Training Program in Stem Cell and Regenerative Developmental Biology (T32 HD007502). T.M.P. and W.P.T. are supported by the National Institutes of Health (CA200709). S.S.H. is supported by the National Institutes of Health (R01DK078640). E.L. is supported by the National Institutes of Health (R01GM081635, R01GM103926 and R35GM122516). Deposited in PMC for release after 12 months.

Supplementary information

Supplementary information available online at
http://jcs.biologists.org/lookup/doi/10.1242/jcs.210575.supplemental

References

Ashkenazi, A. and Dixit, V. M. (1998). Death receptors: signaling and modulation. *Science* **281**, 1305-1308.

Barkett, M., Xue, D., Horvitz, H. R. and Gilmore, T. D. (1997). Phosphorylation of IκB-α Inhibits Its Cleavage by Caspase CPP32 in Vitro. *J. Biol. Chem.* **272**, 29419-29422.

Beurel, E., Grieco, S. F. and Jope, R. S. (2015). Glycogen synthase kinase-3 (GSK3): regulation, actions, and diseases. *Pharmacol. Ther.* **148**, 114-131.

Cole, A. R., Knebel, A., Morrice, N. A., Robertson, L. A., Irving, A. J., Connolly, C. N. and Sutherland, C. (2004). GSK-3 phosphorylation of the Alzheimer epitope within collapsin response mediator proteins regulates axon elongation in primary neurons. *J. Biol. Chem.* **279**, 50176-50180.

Damgaard, R. B., Nachbur, U., Yabal, M., Wong, W. W.-L., Fiil, B. K., Kastirr, M., Rieser, E., Rickard, J. A., Bankovacki, A., Peschel, C. et al. (2012). The ubiquitin ligase XIAP recruits LUBAC for NOD2 signaling in inflammation and innate immunity. *Mol. Cell* **46**, 746-758.

Daniels, D. L. and Weis, W. I. (2005). Beta-catenin directly displaces Groucho/TLE repressors from Tcf/Lef in Wnt-mediated transcription activation. *Nat. Struct. Mol. Biol.* **12**, 364-371.

Galbán, S. and Duckett, C. S. (2010). XIAP as a ubiquitin ligase in cellular signaling. *Cell Death Differ.* **17**, 54-60.

Gyrd-Hansen, M., Darding, M., Miasari, M., Santoro, M. M., Zender, L., Xue, W., Tenev, T., da Fonseca, P. C. A., Zvelebil, M., Bujnicki, J. M. et al. (2008). IAPs contain an evolutionarily conserved ubiquitin-binding domain that regulates NF-kappaB as well as cell survival and oncogenesis. *Nat. Cell Biol.* **10**, 1309-1317.

Hanson, A. J., Wallace, H. A., Freeman, T. J., Beauchamp, R. D., Lee, L. A. and Lee, E. (2012). XIAP monoubiquitylates Groucho/TLE to promote canonical Wnt signaling. *Mol. Cell* **45**, 619-628.

Heasman, J. (2006). Patterning the early Xenopus embryo. *Development* **133**, 1205-1217.

Holley, C. L., Olson, M. R., Colón-Ramos, D. A. and Kornbluth, S. (2002). Reaper eliminates IAP proteins through stimulated IAP degradation and generalized translational inhibition. *Nat. Cell Biol.* **40**, 439-444.

Hornbeck, P. V., Zhang, B., Murray, B., Kornhauser, J. M., Latham, V. and Skrzypek, E. (2015). PhosphoSitePlus, 2014: mutations, PTMs and recalibrations. *Nucleic Acids Res.* **43**, D512-D520.

Laible, M. and Boonrod, K. (2009). Homemade site directed mutagenesis of whole plasmids. *J. Vis. Exp.* **27**, e1135.

Liu, C., Li, Y., Semenov, M., Han, C., Baeg, G.-H., Tan, Y., Zhang, Z., Lin, X. and He, X. (2002). Control of beta-catenin phosphorylation/degradation by a dual-kinase mechanism. *Cell* **108**, 837-847.

Macfarlane, M., Merrison, W., Bratton, S. B. and Cohen, G. M. (2002). Proteasome-mediated degradation of Smac during apoptosis: XIAP promotes Smac ubiquitination in vitro. *J. Biol. Chem.* **277**, 36611-36616.

Mertins, P., Mani, D. R., Ruggles, K. V., Gillette, M. A., Clauser, K. R., Wang, P., Wang, X., Qiao, J. W., Cao, S., Petralia, F. et al. (2016). Proteogenomics connects somatic mutations to signalling in breast cancer. *Nature* **534**, 55-62.

Muratani, M. and Tansey, W. P. (2003). How the ubiquitin–proteasome system controls transcription. *Nat. Rev. Mol. Cell Biol.* **4**, 192-201.

Peng, J. (1991). Appendix A: Solutions and Protocols. Methods in Cell Biology. In *Xenopus laevis: Practical Uses in Cell and Molecular Biology*. Elsevier BV.

Saito-Diaz, K., Chen, T. W., Wang, X., Thorne, C. A., Wallace, H. A., PAGE-Mccaw, A. and Lee, E. (2013). The way Wnt works: components and mechanism. *Growth Factors* **31**, 1-31.

Salghetti, S. E., Kim, S. Y. and Tansey, W. P. (1999). Destruction of MYC by ubiquitin-mediated proteolysis: cancer-associated and transforming mutations stabilize MYC. *EMBO J.* **18**, 717-726.

Sharma, K., D'souza, R. C. J., Tyanova, S., Schaab, C., Wiśniewski, J. R., Cox, J. and Mann, M. (2014). Ultradeep human phosphoproteome reveals a distinct regulatory nature of Tyr and Ser/Thr-based signaling. *Cell Rep.* **8**, 1583-1594.

Sun, M., Meares, G., Song, L. and Jope, R. S. (2009). XIAP associates with GSK3 and inhibits the promotion of intrinsic apoptotic signaling by GSK3. *Cell. Signal.* **21**, 1857-1865.

Suzuki, Y., Nakabayashi, Y. and Takahashi, R. (2001). Ubiquitin-protein ligase activity of X-linked inhibitor of apoptosis protein promotes proteasomal degradation of caspase-3 and enhances its anti-apoptotic effect in Fas-induced cell death. *Proc. Natl Acad. Sci. USA* **98**, 8662-8667.

Thorne, C. A., Hanson, A. J., Schneider, J., Tahinci, E., Orton, D., Cselenyi, C. S., Jernigan, K. K., Meyers, K. C., Hang, B. I., Waterson, A. G. et al. (2010). Small-molecule inhibition of Wnt signaling through activation of casein kinase 1alpha. *Nat. Chem. Biol.* **6**, 829-836.

Veeman, M. T., Slusarski, D. C., Kaykas, A., Louie, S. H. and Moon, R. T. (2003). Zebrafish prickle, a modulator of noncanonical Wnt/Fz signaling, regulates gastrulation movements. *Curr. Biol.* **13**, 680-685.

Wu, D. and Pan, W. (2010). GSK3: a multifaceted kinase in Wnt signaling. *Trends Biochem. Sci.* **35**, 161-168.

Zeng, X., Tamai, K., Doble, B., Li, S., Huang, H., Habas, R., Okamura, H., Woodgett, J. and He, X. (2005). A dual-kinase mechanism for Wnt co-receptor phosphorylation and activation. *Nature* **438**, 873-877.